THE ASTROPHYSICAL JOURNAL, 360:20–29, 1990 September 1

H I ABSORPTION TOWARD COOLING FLOWS IN CLUSTERS OF GALAXIES

BRIAN R. MCNAMARA[1,2]
Astronomy Department, University of Virginia
JOEL N. BREGMAN[1,2]
National Radio Astronomy Observatory, and Astronomy Department, University of Michigan
AND
ROBERT W. O'CONNELL[1]
Astronomy Department, University of Virginia
Received 1989 December 1; accepted 1990 March 2

ABSTRACT

We present the results of a search for neutral hydrogen in 14 cooling flow and two non–cooling flow clusters of galaxies with the Arecibo 1000 foot and Green Bank 300 foot radio telescopes. H I was detected in absorption against the radio continuum sources of two (2A0335+096 and MKW3s) centrally dominant, cooling flow cluster galaxies (CFDs). The absorption features have column densities of $N_{\rm H\,I} = 2\text{–}3 \times 10^{20}$ $(T_s/100\ {\rm K})^{-1}\ {\rm cm}^{-2}$, widths of $\Delta V_{\rm FWHM} \sim 30\text{–}100$ km s^{-1}, and optical depths of a few percent. The H I absorption features are redshifted with respect to the CFDs by $\sim$100–250 km s^{-1}, indicating that the H I is probably falling into the CFDs. The H I in MKW3s appears to be located at a projected distance of $\sim$70 kpc from the nucleus of the CFD. H I was not detected in emission; the mean H I upper limit for the sample is $M_{\rm H\,I} \lesssim 6 \times 10^9\ M_\odot$ of optically thin H I, but the limit based on the most sensitive observations is $M_{\rm H\,I} \lesssim 2 \times 10^8\ M_\odot$. Upper limits to the H I to dust ratio in four CFDs are consistent with the Galactic mean gas-to-dust ratio ($M_g/M_d \sim 100$). The emission limits suggest that the optically thin H I is confined to 8–15 kpc regions about the radio sources. If the H I is in pressure equilibrium with the high-temperature and high-pressure X-ray plasma, then the H I clouds are orders of magnitude smaller, denser, and less massive than their Galactic counterparts. The small amount of H I and the large star formation rate observed in 2A 0335+096 suggest that star formation occurs more rapidly and efficiently than in disk galaxies. The origin of the H I cannot be determined with certainty, but the large cooling rates in the detected CFDs ($\langle \dot{m}_{\rm CF} \rangle_{\rm det} = 250\ M_\odot\ {\rm yr}^{-1}$) compared to the mean for the CFDs that were not detected ($\langle \dot{m}_{\rm CF} \rangle_{\rm nd} = 106\ M_\odot\ {\rm yr}^{-1}$) suggests that the H I originated from the cooling flows. These observations, together with the recent detections of H I and CO in NGC 1275, constitute the most direct evidence to date that the intracluster gas is accreting onto the CFDs and cooling to temperatures low enough for star formation to occur.

Subject headings: accretion — galaxies: clustering — galaxies: structure — radio sources: 21 cm radiation

I. INTRODUCTION

X-ray imaging of clusters of galaxies has revealed the presence of hot ($T \sim 3 \times 10^7$–10^8 K) gas whose mass is comparable to or greater than the sum of the constituent galaxies (see Forman and Jones 1982; Sarazin 1986). The radiative cooling time is often less than the Hubble time in the inner 100–200 kpc of the clusters, resulting in an inferred accretion rate of $\sim 100\ M_\odot\ {\rm yr}^{-1}$ of cool gas onto the central dominant galaxies near the cluster centers (see Sarazin 1986; Fabian 1988). Most of the cluster cooling flow galaxies discussed here are cD galaxies; however, we refer to central dominant galaxies at the centers of cooling flow clusters as "cooling flow dominant" or CFD galaxies to avoid any question of their strict morphological type.

The large mass accretion rates, $\dot{m}_{\rm CF}$, inferred from the X-ray data imply that substantial amounts of accumulated gas and/or vigorous star formation should be present in CFDs. Unusually strong nuclear emission lines, extended emission-line structures, and extended blue colors associated with recent or ongoing star formation have been reported in $\sim$50% of well-studied CFDs. The CFDs with the largest cooling rates tend to show the most prominent effects (Heckman 1981; Cowie *et al.* 1983; Hu, Cowie, and Wang 1985; Johnstone, Fabian, and Nulsen 1987; Romanishin 1987; Heckman *et al.* 1989; McNamara and O'Connell 1989). However, at the inferred cooling rates, typically $\lesssim$1% of the accreted material can be accounted for in warm gas or star formation with the Galactic, or "local," initial mass function (IMF). Therefore, a population of very low mass stars ($\ll 1\ M_\odot$) appears to be the most viable final state of the cooling material (Fabian, Nulsen, and Canizares 1982; Sarazin and O'Connell 1983; O'Connell and McNamara 1989). If most of the material is indeed deposited in stars, the cooling gas should pass through a neutral stage prior to star formation (Bregman, Roberts, and Giovanelli 1988) and could be detectable in the 21 cm line feature of neutral hydrogen (H I).

Previous searches for H I in cD galaxies (Burns, White, and Haynes 1981; Valentijn and Giovanelli 1982) failed to detect H I. Three objects in these surveys were CFDs with $\dot{m}_{\rm CF} < 50\ M_\odot\ {\rm yr}^{-1}$. However, H I absorption features have been detected against the nuclear continuum source of NGC 1275/Perseus at

[1] Visiting Astronomer, Arecibo Observatory, National Astronomy and Ionosphere Center; the NAIC is operated by Cornell University under contract with the National Science Foundation.

[2] Visiting Astronomer, National Radio Astronomy Observatory, which is operated by Associated Universities, Inc., under contract with the National Science Foundation.

the velocity of the cluster's high-velocity filament system (De Young, Roberts, and Saslaw 1973) and at the stellar velocity of NGC 1275 as well (Crane, van der Hulst, and Haschick 1982; Jaffe, de Bruyn, and Sijbreng 1988). Although OH absorption was not detected (O'Dea and Baum 1987), Lazareff *et al.* (1989) and Mirabel, Sanders, and Kazes (1989) recently detected CO in emission at a velocity nearly coincident with the stellar velocity of NGC 1275. This molecular gas, which may be related to the low-velocity optical filaments, is estimated to have mass of $\sim 6 \times 10^9 M_\odot$.

The detections of H I and CO in NGC 1275 were the first indications that cool gas, which may have originated in a cluster cooling flow, is present in a CFD galaxy. However, a search for H I in a large sample of CFDs had not been conducted. Therefore, we have undertaken a new H I survey of cluster cooling flows with the Arecibo 1000 foot and Green Bank 300 foot telescopes. The H I absorption results presented here, in addition to the recent observations of NGC 1275, provide the strongest evidence to date for the presence of cool gas associated with cooling flows.

All distance-dependent quantities presented here assume $H_0 = 50 \text{ km s}^{-1} \text{ Mpc}^{-1}$.

II. OBSERVATIONS

a) *The Sample*

Our sample objects were chosen primarily from the Arnaud and Fabian (1989) catalog of cooling flow clusters observed with the *Einstein* X-ray observatory, with the exception of 2A 0335+096, which was taken from the compilation of Sarazin (1986). Objects with the largest mass accretion rates and the smallest distances were allotted most of the observing time, but a small sample of clusters with $\dot{m}_{CF} \sim 0$–$10\ M_\odot\ \text{yr}^{-1}$ was included. Though H I was detected only in absorption, our sample selection criterion did not consider the radio continuum properties of the CFDs.

b) *Arecibo Observations*

Observations were made with the Arecibo 1000 foot telescope during 1987 October 4–15 and 1988 March 31–April 10. Most of the observations were conducted at night to take advantage of the better baselines. (1988 April daytime observations of 2A 0335+096 were also obtained.) We used the 12 m line feed, which collects two circular polarizations of 21 cm radiation; observations were carried out in the total power mode. The back end consisted of the 20 MHz bandwidth autocorrelation spectrograph with 2048 channels divided into four 512 channel subcorrelators (two per polarization), giving typically 9 km s^{-1} resolution per channel. The half-power beam size is $3'.3 \pm 0'.1$, and typical system temperatures were 35–40 K; the gain was 8 K Jy^{-1}. The bandpass and telescope beam were centered at the heliocentric velocity and position of the cluster's CFD (if a reliable velocity was not available, the cluster's mean velocity was used).

The detected absorption features are weak, so care was taken to minimize the possibility of spurious instrumental effects. When an emission or absorption feature was suspected, we shifted the central velocity of the receiver by 100–200 km s^{-1} to either side of the standard velocity. Absorption features were considered noninstrumental if they remained at the same velocity in the shifted data. This procedure successfully identified spurious instrumental line features. The individual spectra were then shifted to a common channel-velocity spacing, flux calibrated, weighted by the system temperature, and added to produce the final spectra, using the standard NAIC software.

The most troublesome technical problem encountered at Arecibo was the pervasive ground-based radio frequency (RF) interference that is present at a number of frequencies in the range 1320–1400 MHz. During the spring of 1988 we were generally successful eliminating the interference from the San Juan airport radar with a device that locked onto the radar's frequency and turned off the correlator while the offending radiation was beamed toward the dish. More problematic was the intermittent interference of unknown origin present in the data. When present, these features were generally narrow (two to three channels wide) and usually alternated between emission and absorption in the reduced spectra from consecutive days. The alternating emission-absorption spectrum is due to variations in the flux density of the interference signal in the "on" and "off" spectra. When interference signals were present but were not sufficiently strong to compromise the overall quality of the spectrum, they were included in the final spectrum and the frequency (velocity) of the signal was noted (e.g., Figs. 1 and 2). The final spectra usually show no residual effect due to smoothing by averaging over many individual spectra. By contrast, the features considered to be real H I absorption features *always* appeared in absorption and range from 6–27 channels in width. In addition, a spurious absorption feature in the reduced spectrum will appear as an emission feature in the "off" spectrum. The only absorption feature found to be contaminated by emission in the "off" spectra is the highest velocity feature in MKW3s, indicated in Figure 2. The interference feature in the "off" spectrum was, however, narrower than the absorption feature and did not appear in all of the spectra. Nonetheless, this feature is suspect, so we do not consider it further in this paper.

During the lengthy observing time for 2A 0335+096 in this study and NGC 5846 in Bregman, Roberts, and Giovanelli (1988) the baseline rms decreased as the square root of the integration time over 490 minutes of "on" integration. The final spectra consisted of typically 10–30 5 minute on/off pairs; 77 pairs were obtained for 2A 0335+096.

c) *Green Bank Observations*

The Green Bank 300 foot observations were obtained during 1988 September. The 22 cm autocorrelator provided 200 usable channels at a resolution of ~ 12 km s^{-1} per channel with a total usable bandwidth of ~ 2200 km s^{-1}. The receiver provided a gain of 1 K Jy^{-1} and the system temperature was ~ 20 K; the full width at half-power beam size was $10'$. Spectra were obtained in total power mode, flux calibrated with the standard gain curves, weighted by the system temperature, and combined with the DRAWSPEC data reduction package of H. Liszt.

In a few cases, such as A2151, H I emission features from cluster spirals in the telescope beam contaminated the measurements. When this occurred, the data were discarded.

The problem of standing waves in the instrumental baselines due to radiation reflected off the support structure of the telescope was encountered in objects with continuum sources $\gtrsim 500$ mJy. For those observations in which standing waves occur, the wave structure is broader than the detected H I absorption features. Broad emission or absorption features with flux integrals similar to those in the detected objects would be difficult, if not impossible, to detect without a reliable method of removing the standing waves. We attempted to do

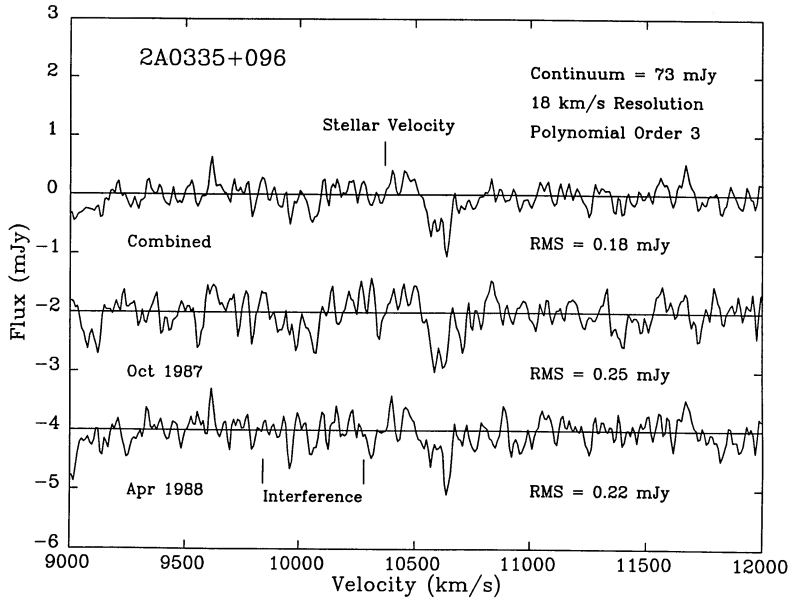

FIG. 1.—The H I absorption-line spectrum for 2A 0335+096, taken with the Arecibo 1000 foot radio telescope, is shown with the baseline subtracted. The top panel is the weighted average of the 1987 October and the 1988 April total power spectra (77 × 5 minute on-off pairs) observed with the Arecibo telescope. The stellar absorption-line velocity is indicated; the gas is falling onto the CFD with a velocity of ~240 km s^{-1}. The location of intermittent, low-level RF interference is indicated and shows no residual effects.

this by fitting sinusoidal waves to the baselines, after polynomial subtraction, of some of the Green Bank spectra. The results were slightly improved upper limits to $M_{\rm H\,I}$; however, no convincing evidence for broad H I emission/absorption features emerged.

We recently reported the detection of an H I absorption feature in A85 and the possible detections of H I absorption in A262 and A376 with the Green Bank 300 foot telescope (McNamara, O'Connell, and Bregman 1989). We have reanalyzed this data, and these features may be attributable to a faulty subcorrelator. Our upper limit on τ for A262 was confirmed by Giovanelli (1989); no absorption feature was found above the 2 σ level.

d) Results

The general results of the survey are presented in Table 1. Columns (1)–(3) identify the cluster, central galaxy, and radio source, respectively. Columns (4) and (5) list the position of the CFD measured with the NRAO Mann measuring engine. Positions less accurate than 0.1 (in right ascension) were

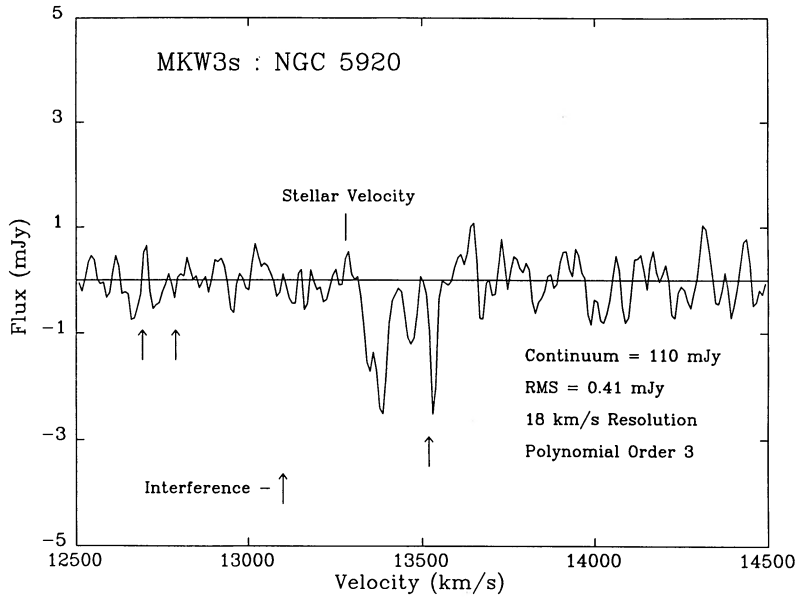

FIG. 2.—The absorption-line spectrum for NGC 5920 in MKW3s, taken with the Arecibo 1000 foot radio telescope, after baseline removal. The stellar absorption-line velocity is indicated; the gas is probably falling onto NGC 5920 with a velocity of at least 90–220 km s^{-1}. The radio-source centroid is displaced by 56″ (69 kpc) to the south-west of NGC 5920, which suggests that the H I absorption clouds are located away from the nucleus. Intermittent, low-level RF interference, which is indicated, had little residual effect. However, the highest velocity absorption feature is contaminated by RF interference and may be spurious.

obtained from the literature and are generally within $\sim 20''$ of the CFD. Velocities for the CFD or cluster presented in column (6) were taken from the literature as listed in the notes to Table 1 and correspond to the center of the bandwidth. The total mass accretion rates, $\dot{m}_{CF}$, taken from Arnaud and Fabian (1989) or Singh, Westergaard, and Schnopper (1988) are listed in column (7). Columns (8)–(11) list the telescope (GB = Green Bank 300 foot telescope and A = Arecibo 1000 foot telescope), the "on" integration time in minutes, the observed continuum flux density, and the rms error of the unsmoothed baselines after polynomial subtraction. Columns (12) and (13), respectively, list the 3 σ upper limits to the optical depth of an absorption feature and H I mass in emission.

The 3 σ detection upper limits to the optical depth of a rectangular absorption feature with an assumed width of $\Delta V_a = 100$ km s^{-1} (similar to the velocity widths of the absorption features in 2A 0335+096 and MKW3s) were computed with expression (1) in Haynes, Brown, and Roberts (1978), which we have generalized for absorption features that are broader than one channel:

$$\tau = \ln\left[1 + \frac{3\sigma_c}{S_c}\left(\frac{\Delta V_c}{\Delta V_a}\right)^{1/2}\right],$$

where σ_c and S_c are taken from Table 1 and ΔV_c is the velocity spacing per channel (~ 9 km s^{-1} for the Arecibo observations and ~ 12 km s^{-1} for the Green Bank observations).

The 3 σ detection upper limits to M_{HI} in emission were computed with the expression from Burns, White, and Haynes (1981), again generalized for emission features that are broader than one channel:

$$M_{HI} = 236D^2 \frac{3\sigma_c \Delta V_e}{\sqrt{\Delta V_e/\Delta V_c}} M_\odot ,$$

where ΔV_e is the assumed emission-line velocity width of 300 km s^{-1}, and D is the cluster's distance in Mpc. It is difficult to estimate the emission-line velicity width, ΔV_e (see Burns, White, and Haynes 1981), so we adopt 300 km s^{-1}, which is a characteristic stellar velocity dispersion for cD galaxies. Cluster distances were computed with the CFD or mean velocities taken from the references listed in the notes to Table 1 and corrected to Local Group velocities ($V_{lg} = V_\odot + 300 \sin l \cos b$) when necessary.

Although there were no detections in emission, H I absorption was detected toward 2A 0335+096 and MKW3s at $\gtrsim 6\ \sigma$ significance (Figs. 1 and 2; Table 2). The absorption spectra, presented in Figures 1 and 2, were Hanning smoothed to a velocity resolution of 18 km s^{-1}. Instrumental baselines were removed by fitting polynomials to the continuum, avoiding the absorption features. In all cases, the baselines were smoothly varying, and polynomials no higher than third order were necessary. The measured absorption-line maximum optical depths, τ_0 (not the same as Table 1, col [12]), flux integrals, and column densities [$N_{HI} = 1.823 \times 10^{20}(T_s/100\ \mathrm{K})^{-1} \int \tau\, dv\ \mathrm{cm}^{-2}$], that are presented in Table 2, columns (2)–(4), respectively, are insensitive to the order of the polynomial. The errors for the absorption-line flux integrals were computed following Lockman, Jahoda, and McCammon (1986) as:

$$\sigma_{fi} = \sigma_c \Delta V_c \left[\left(\frac{\Delta V_l}{\Delta V_c}\right) + \frac{1}{N_{bl}}\left(\frac{\Delta V_l}{\Delta V_c}\right)^2\right]^{1/2} \mathrm{mJy\ km\ s^{-1}} ,$$

where N_{bl} is the number of baseline channels over which the polynomial was fit and ΔV_l is the full velocity width of the line. Columns (5)–(7) in Table 2 list the full width at half-maximum of the absorption features, ΔV_{FWHM}, the full velocity width at the continuum, ΔV_{FW}, and the mean heliocentric velocity of

TABLE 1

CLUSTERS OBSERVED

Cluster (1)	CFD (2)	Radio Source (3)	R.A. (1950) (4)	Decl. (1950) (5)	V (km s^{-1}) (6)	$\dot{m}_{CF}$ ($M_\odot$ yr^{-1}) (7)	Telescope (8)	t_{int}[a] (minutes) (9)	S_c (mJy) (10)	σ_c (mJy) (11)	τ[b] (12)	M_{HI}[c] ($10^9\ M_\odot$) (13)
A119	...	...	$00^h53^m51^s$	$-01°32'02''$	13101[d]	0	GB	48	1670	4.53	<0.0028	<13
A262	N708	B2.3 0149+35[e]	01 49 50.0	+35 54 22	4887[f]	47	GB	44	108	2.70	<0.0250	<1.2
A376	...	...	02 42 40	+36 39 22	14660[d]	92	GB	24	57	2.56	<0.0458	<9.4
AWM7	N1129	...	02 51 12.8	+41 22 36	5396[d]	41	GB	40	148	4.20	<0.0283	<2.2
A400	...	3C 75	02 55 03.1	+05 49 30	6955[d]	7	A	105	3630	1.66	<0.0004	<1.2
2A 0335+096	...	...	03 35 57.4	+09 48 28	10368[g]	200[h]	A	385	73	0.28	0.0035	<0.44
A496	...	MSH 04-112[e]	04 31 18.7	−13 21 56	9802[i]	101	GB	40	287	2.99	<0.0106	<4.7
A1142	...	...	10 58 20.0	+10 46 29	11183[j]	4	A	85	50	0.44	<0.0078	<0.80
MKW4[k]	N4073	...	12 01 53.3	+02 10 27	5936[f]	22	A	175	10	0.48	<0.0413	<0.23
A1795	...	4C 26.42	13 46 34.0	+26 50 28	19067[f]	295	A	110	1228	1.00	<0.0007	<5.2
A1991	N5778	...	14 52 13.1	+18 50 40	17958[f]	71	A	40	70	0.74	<0.0096	<3.6
A2029	...	...	15 08 27.2	+05 55 55	23474[f]	366	A	60	680	1.26	<0.0017	<11
A2040	...	...	15 10 20	+07 37 42	13671[d]	0	A	10	<10	1.12	...	<3.1
A2052	...	3C 317	15 14 17.0	+07 12 14	10253[f]	127	A	90	12600	22.64	<0.0016	<35
MKW3s	N5920	3C 318.1	15 19 25.3	+07 53 13	13281[f]	151	A	170	110	0.65	0.0067	<1.7
A2063	...	...	15 20 39	+08 47 12	10103[d]	45	A	40	13	0.64	<0.0429	<0.95

[a] "On" integration time for total power observations.
[b] Three sigma upper limits for the nondetected objects are based on an assumed absorption-line width of 100 km s^{-1}.
[c] Three sigma upper limits are based on an assumed emission-line width of 300 km s^{-1}.
[d] Galactocentric cluster velocity from Struble and Rood 1987.
[e] Hu, Cowie, and Wang 1985.
[f] Heliocentric velocity of the CFD from McNamara and O'Connell 1989.
[g] Heliocentric velocity of the CFD from Huchra (private communication).
[h] $\dot{m}_{CF}$ from Singh, Westergaard, and Schnopper 1988.
[i] Heliocentric velocity of the CFD from Kriss *et al.* 1989.
[j] Cluster redshift from Zhao, Burns, and Owen 1989.
[k] Strong interference in the H I spectrum near the stellar absorption-line velocity.

TABLE 2

H I Absorption-Line Detections

Cluster (1)	τ_0 (2)	$\sum f\Delta V$ (mJy km s^{-1}) (3)	$N_{\rm H\,I}$ (10^{20} cm^{-2} T_{100}^{-1}) (4)	$\Delta_{V_{\rm FWHM}}$ (km s^{-1}) (5)	$\Delta V_{\rm FW}$ (km s^{-1}) (6)	$V_{\rm H\,I}$ (km s^{-1}) (7)	$V_* - V_{\rm H\,I}$ (km s^{-1}) (8)
2A 0335+096	0.014	69 ± 8.97	1.74	96	147	10,605	−237
2A 0335+096[a]	...	87 ± 12.7	2.18	...	274	...	...
MKW3s	0.023	142 ± 17.9	2.38	62	117	13,371	−90
	0.011	44 ± 12.7	0.72	35	62	13,504	−223

[a] Measurements include the red wing of the 2A 0335+096 absorption line.

the absorbing H I, $V_{\rm H\,I}$, respectively. The velocity difference between $V_{\rm H\,I}$ and the heliocentric stellar absorption-line velocity of the CFD, V_*, is listed in column (8). The spectral line analysis was done with software developed at Virginia for the VAX-IDL image processing system.

III. PROPERTIES OF CFD GALAXIES WITH H I IN ABSORPTION

We have detected H I in absorption against the nuclear radio continuua of MKW3s and 2A 0335+096. Since H I absorption has been detected previously in only one other CFD (NGC 1275), we summarize here their X-ray, optical, and radio properties, to complement the discussion in § IV.

a) 2A 0335+096

2A 0335+096 (Zw 0335.1+0956) is a medium-compact cluster of galaxies with at least 97 member galaxies. The cluster is a luminous X-ray source ($L_x = 1.5 \times 10^{44}$ ergs s^{-1}, 2–6 keV), with a high central electron density ($n_0 = 23 \times 10^{-3}$ cm^{-3}) and a short cooling time, resulting in a inferred cooling radius of $R_{\rm cool} \sim 150$ kpc and a mass-accretion rate of $\dot{m}_{\rm CF} \sim 200\ M_\odot$ yr^{-1} (Schwartz, Schwarz, and Tucker 1980; Mushotzky and Szymkowiak 1988; Westergaard 1988; Singh, Westergaard, and Schnopper 1988).

2A 0335+096 is a typical example of a cluster cooling flow with extended emission-line filaments and vigorous star formation in its central galaxy—similar to NGC 1275. CCD images of the CFD show a color profile in the inner 6″–35″ (6–35 kpc) that is bluer than a normal gE (Romanishin and Hintzen 1988). The extended blue color is attributed to star formation at the rate of $S \sim 8\ M_\odot$ yr^{-1} (assuming the local IMF), which is presumably fueled by the cooling flow. A dust lane in the inner 6″ causes noticeable reddening, with an estimated color excess of $E(B-V) \sim 0.2$. There is a small, faint ($M_R \sim 18.5$) elliptical-like companion galaxy projected against the CFD 6″ (6 kpc) to the north-east of the CFD's nucleus (Romanishin and Hintzen 1988). We know of no available radial velocity measurements for the companion galaxy, so its relationship to the CFD is not known.

The radio continuum source in 2A 0335+096 appears to be a point source coincident with the CFD, based on a C-array VLA map at 1452 MHz (O'Dea, Baum, and Killeen 1987). However, they found a flux density for the point source of only 15 mJy, whereas we found a 73 mJy source. Based on synthesis maps of the other radio sources in this cluster (O'Dea and Owen 1985; Patnaik and Singh 1988) and the sidelobe map for the Arecibo telescope (Haynes and Giovanelli 1984), the larger flux density that we find cannot be due to sidelobe contamination. However, the discrepancy may be attributable to the difficulty detecting extended low surface brightness emission with the VLA and Ooty synthesis telescopes.

The H I spectrum of 2A 0335+096 (Fig. 1) shows a weak absorption feature with a maximum optical depth $\tau_0 = 0.014$ and a full velocity at the baseline of $\Delta V_{\rm FW} = 147$ km s^{-1}. The absorption feature apparently has a red wing, which is evident in both the 1987 October and 1988 April spectra. This is a commonly observed characteristic of H I absorption features in early-type galaxies (e.g., Van Gorkom *et al.* 1989).

There is little evidence for an H I emission feature in Figure 1 (other than a narrow 3 σ feature located near the indicated stellar velocity). Assuming this weak emission is not real, the upper limit to the H I mass (see Table 1) is $M_{\rm H\,I} < 4.4 \times 10^8\ M_\odot$, assuming the H I is optically thin.

The radial extent of the H I can be roughly estimated from the H I upper limit and the column density of the absorption feature, assuming the radio source is covered by spherically distributed H I, using:

$$R_{\rm H\,I} \sim \left(\frac{3M_{\rm H\,I}}{\alpha 4\pi m_{\rm H} N_{\rm H\,I}}\right)^{1/2} \sim 8\left(\frac{\alpha T_s}{100\ {\rm K}}\right)^{-1/2}\ {\rm kpc}\,,$$

where $m_{\rm H}$ is the mass of the hydrogen atom, T_s is the spin temperature, and α is the fraction of the projected area within $R_{\rm H\,I}$ that is covered. We cannot assess α based on this data, although the error introduced into $R_{\rm H\,I}$ for $\alpha < 1$ will be partially offset by the use of upper limits for $M_{\rm H\,I}$. If the inferred extended radio source is not covered by the H I, then our column densities are lower limits, and $R_{\rm H\,I}$ could be considerably smaller. The size of this effect, however, cannot be assessed without a high signal-to-noise H I map.

$R_{\rm H\,I}$ is comparable to the size of the dust lane. If the H I absorption feature and the dust are coextensive, then a comparison of these observations establishes a relationship between the spin temperature and the gas-to-dust ratio. Using the relationship between extinction and column density given by Savage and Mathis (1979), we find that $T_s \sim 440[(M_g/M_d)/100]$ K, which is typical of Galactic values (Kulkarni and Heiles 1988).

The H I appears to be falling into the CFD at $\Delta V \equiv V_* - V_{\rm H\,I} = -237$ km s^{-1}. Unless the H I has a large tangential velocity, it is bound to the galaxy, since its velocity shift is less than the escape velocity of the galaxy, which is $\sim 2 \times 3^{1/2}\sigma_V$, where σ_V is the stellar velocity dispersion ($\sigma_V = 255$ km s^{-1}; Huchra 1989). The velocity width of the absorption feature is far greater than the thermal width of neutral hydrogen (the temperature implied by the velocity width would exceed the ionization temperature of H I), indicating that the absorbing H I lies in many individual cloud structures along the line of sight.

b) MKW3s

MKW3s (Zw 1518.8+0747) is a medium-compact, spiral-poor cluster of galaxies containing the centrally dominant galaxy NGC 5920. The cluster has a smooth, symmetric and centrally peaked X-ray profile that is morphologically similar to BM I clusters (Kriss *et al.* 1980). The X-ray luminosity of the cluster ($\sim 1 \times 10^{44}$ ergs s^{-1}, 0.1–3 keV) and central electron density ($n_0 = 5 \times 10^{-3}$ cm^{-3}) imply a short radiative cooling time ($t_{\rm cool} = 0.4$ Gyr), a inferred cooling radius $R_{\rm cool} \sim 210$ kpc, and a mass-accretion rate of $\dot{m}_{\rm CF} \sim 151\ M_\odot\ {\rm yr}^{-1}$ (Canizares, Stewart, and Fabian 1983; Arnaud and Fabian 1989).

Synthesis maps of the radio source (3C 318.1) at 1407 MHz show the steep-spectrum source ($\alpha = -2.7$; $S_c = 90 \pm 20$ mJy) to be displaced by 56″ (69 kpc) to the south-west of NGC 5920 (Slingo 1974). Our continuum measurement ($S_c = 110$ mJy) agrees with Slingo's value, so it appears that this source contributes most of the flux to our H I spectrum. Only a weak radio source (2.1 mJy at 4850 MHz) is found at the position of the CFD (O'Dea, Baum, and Killeen 1987).

Our Arecibo spectrum (Fig. 2) shows three absorption features against the 110 mJy continuum source; the H I is probably projected against the peak of steep-spectrum radio source. The highest velocity component is contaminated with radio interference and may be spurious (see § II*b*), so flux measurements for only the lower velocity features are presented in Table 2. The absorption features are redshifted with respect to the stellar velocity of NGC 5920 by $\Delta V \sim -90$ to -225 km s^{-1}, similar to the result for 2A 0335+096. The velocity width at the baseline continuum for the absorption features is ~ 180 km s^{-1} wide, which again indicates many individual H I cloud structures along the line of sight. We know of no stellar velocity dispersion measurement for NGC 5920; however, the mean velocity dispersion for poor-cluster cD galaxies (Malumuth and Kirshner 1985) is $\sigma_v = 287 \pm 64$ km s^{-1}, so the H I is probably bound to the CFD, unless it has a large tangential velocity.

Since the absorbing H I is unlikely to be near the core of NGC 5920, a cylinder covering the radio source may be a reasonable approximation to the geometry of the H I region. Using the H I mass upper limit in Table 1 and the column density of the absorption features, the characteristic size of the H I covering the radio source is:

$$R_{\rm H\,I} \sim \left(\frac{M_{\rm H\,I}}{\alpha \pi m_{\rm H} N_{\rm H\,I}}\right)^{1/2} \sim 15 \left(\frac{\alpha T_s}{100\ {\rm K}}\right)^{-1/2}\ {\rm kpc}\ .$$

We have made similar assumptions as those for 2A 0335+096; however, the column density in this case is almost certainly a lower limit, since the radio source is extended with dimensions as large as 39 × 116 kpc (Slingo 1974).

If the H I is distributed throughout the hot atmosphere, it is likely to be spherically distributed about the CFD to radii $\lesssim R_{\rm cool}$. The displacement of the radio source from the nucleus of NGC 5920 implies that the projected H I is at a radius $R_{\rm H\,I} \gtrsim 70$ kpc $\gtrsim 1/3 R_{\rm cool}$, which is consistent with the model. If $\alpha \sim 1$, the implied optically thin H I mass within the area bounded by $R_{\rm H\,I}$ is $M_{\rm H\,I} \sim 4 \times 10^{10} (T_s/100\ {\rm K})\ M_\odot$. This exceeds the upper limit in Table 1. Therefore, unless α is small and the H I fortuitously just covers the radio source, the H I is probably opaque. If true, this would be important because it implies quantities of H I that could greatly exceed the upper limits in Table 1 (which assume that $\tau \ll 1$) may be present in MKW3s and perhaps in other cooling flow clusters as well.

The other CFDs with H I absorption (2A 0335+096, NGC 1275) have ongoing or recent high-mass star formation as inferred from their blue colors. However, NGC 5920 has normal broad-band colors [$(B-V)_T^0 = 0.89$; RC2], and detailed spectrophotometry shows no evidence for a young stellar population (Johnstone, Fabian, and Nulsen 1987; McNamara and O'Connell 1989). The galaxy has a 4.6 Å equivalent width [O II] λ3727 emission line, which is slightly larger than the mean for E/S0's, though it is not unusual (see Caldwell 1984).

IV. DISCUSSION

a) Estimated Properties of the H I Absorption Clouds

As discussed earlier, the H I absorption features have velocity widths that are too broad to be due to a single, thermally broadened cloud. If the observed absorption profiles are due to a number of optically thin H I clouds with different infall velocities but similar spin temperatures and column densities (see Spitzer 1978), then

$$N_{\rm cloud} \gtrsim \frac{\Delta V_{\rm FWHM}}{2\sqrt{\ln 2}} \left(\frac{2kT_s}{m_{\rm H}}\right)^{-1/2} \gtrsim 45 \left(\frac{T_s}{100\ {\rm K}}\right)^{-1/2}$$

clouds lie along the line of sight toward MKW3s and 2A 0335+096. If these clouds are in pressure equilibrium with the hot ambient medium so that $n_s T_s = n_0 T_x$, and the cloud density is $n \sim 7 \times 10^3 (T_s/100\ {\rm K})^{-1}$ cm^{-3}, then the radius of an individual cloud is:

$$R_{\rm cloud} \sim 3.5 \times 10^{-4} \left(\frac{N_{\rm H\,I}}{10^{20}\ {\rm cm}^{-2}}\right) \left(\frac{T_s}{100\ {\rm K}}\right)^{3/2} \times \left(\frac{\Delta V_{\rm FWHM}}{100\ {\rm km\ s}^{-1}}\right)^{-1} \left(\frac{n_0}{10^{-2}\ {\rm cm}^{-3}}\right)^{-1} \left(\frac{T_x}{10^7\ {\rm K}}\right)^{-1}\ {\rm pc}\ ,$$

where $\Delta V_{\rm FWHM}$ and $N_{\rm H\,I}$ for the absorption features are listed in Table 2, and the central electron densities, n_0, and temperatures, T_x, of the X-ray plasma are given in § III. The typical H I cloud has a mass that is $\ll 1\ M_\odot$ for spin temperatures $\lesssim 1000$ K.

By comparison, the clumps of absorbing H I in our Galaxy have densities of ~ 20–50 cm^{-3} and spin temperatures between 30 and 80 K. H I complexes enveloping H II regions have typical volume-average densities of 2.5 cm^{-3}, linear diameters of ~ 120 pc, and masses which are typically $\sim 1 \times 10^5\ M_\odot$ (Kulkarni and Heiles 1988). Therefore, if the H I in CFDs is in thermal pressure equilibrium with the surrounding X-ray plasma with spin temperatures typical of those found in Galactic H I clouds ($T_s \sim 50$–1000 K), then these clouds must be much smaller and denser than their Galactic counterparts.

b) The Origin of H I in Cluster Cooling Flows

There are apparently three potential sources for the absorbing H I gas: the H I may have been stripped from another cluster galaxy by ram pressure or a tidal encounter with the CFD; the H I may be the cool remains of stellar mass loss from red giant stars; or the H I may have originated from the cooling flow.

If the H I were due to ram pressure stripping of H I–rich galaxies by the dense intracluster medium, one might expect the H I to be distributed throughout the cluster's core. The H I is apparently confined to a 10–20 kpc region about the nucleus of 2A 0335+096, but it could be located at least 70 kpc from the nucleus of MKW3s (see § III), whereas a typical cluster

core radius is 150–250 kpc. Since the H I is apparently confined to small areas compared to the area of a cluster core, stripping seems to be an unlikely origin for the H I. Alternatively, the H I could have been tidally stripped from a passing galaxy. The CFD in 2A 0335+096 has a companion at a projected distance that is comparable to the H I radius (see § III*a*); however, this object appears to be a dwarf elliptical which is an unlikely H I donor. In addition, no fewer than seven of the rich cluster CFDs in this sample have potential donor galaxies projected within 10–20 kpc (see Lauer 1989), yet none of these CFDs have H I absorption features. Stripping mechanisms cannot be dismissed as the source of the H I, but there is currently little evidence to support a case for these processes.

Another potential source of cool gas in CFDs is the material that has been returned to the interstellar medium from red giant stars. The mass-return rate should then be proportional to the galaxy's optical luminosity, which for a typical CFD or cD (which have larger luminosities than Es and most gEs), should be $\sim 1\ M_\odot\ \mathrm{yr}^{-1}$ (Faber and Gallagher 1976). However, no correlation has been found between the optical luminosity and $M_{\mathrm{H\,I}}$ in E and gE galaxies (see Knapp, Turner, and Cunniffe 1985). In addition, apart from the CFDs discussed here, H I has not been detected in luminous cDs, which should have the largest mass-return rates. Although there is strong evidence for a relationship between the mass-return rate and the hot interstellar medium in early-type galaxies, a relationship between the mass-return rate and the presence of H I is unsupported.

The third possibility is that the H I originated from the cooling flow. To assess this, we will consider only those objects listed in Table 1 and from Jaffe, de Bruyn, and Sijbreng (1988) that have nuclear continuum sources and optical depth upper limits $\tau < 0.03$. This avoids those objects that could have absorption features as strong as those in 2A 0335+096 and MKW3s but would not have been detected. Of the 13 objects (including NGC 1275; Jaffe, de Bruyn, and Sijbreng 1988) that fit this criterion, the 10 nondetected objects have $\langle \dot{m}_{\mathrm{CF}} \rangle_{\mathrm{nd}} = 106\ M_\odot\ \mathrm{yr}^{-1}$, while the three CFDs (2A 0335+096, MKW3s, and NGC 1275) with H I absorption features have $\langle \dot{m}_{\mathrm{CF}} \rangle_{\mathrm{det}} = 250\ M_\odot\ \mathrm{yr}^{-1}$ (for NGC 1275 we take $\dot{m}_{\mathrm{CF}} = 400\ M_\odot\ \mathrm{yr}^{-1}$; White and Sarazin 1988).

An assessment of why some clusters with large mass-accretion rates were detected while others were not is complicated by the unknown extent to which H I clouds, if present, cover the radio source (i.e., the covering factor). If H I is present in many of the objects sampled but with a covering factor that is considerably less than unity, then the detection of only two objects is not surprising. Furthermore, the radio source morphologies are often spatially extended over tens of kiloparsecs (see Zhao, Burns, and Owen 1989) which could either enhance or lessen the probability of detecting H I in absorption depending, again, on the covering factor. If H I is present but does not completely cover the radio source, the absorption features may be weakened beyond detectability by continuum radiation from regions of the radio source that are not covered by H I. Nonetheless, based on the limited number of observations, the CFDs with H I absorption features appear to distinguish themselves from the remaining sample by their large mass-accretion rates. A firm conclusion awaits a study of a more complete sample of CFDs.

c) Comparison of the H I *Properties to a Cooling Flow Model*

The analysis of cluster cooling flows with spatially resolved X-ray images suggests that $\dot{m}(R) \propto R^n$, where $\dot{m}$ is the total mass flux of cooling material crossing a shell of radius R; typically $n \sim 1$ (Thomas, Fabian, and Nulsen 1987; White and Sarazin 1988). This implies that hot gas is being converted to cold gas over a region extending out to the cooling radius, $R_{\mathrm{cool}} \sim 100$–$200$ kpc. Placing strong constraints on $\dot{m}(r)$ with H I observations depends critically on the fraction of the cooling gas that becomes optically thin H I and the length of time the gas remains in the H I phase; neither quantity is known. If all the cooling material becomes H I, then the amount deposited within a projected H I radius, $R_{\mathrm{H\,I}}$, centered on the CFD is:

$$\dot{m}(R_{\mathrm{H\,I}}) \sim \frac{\pi}{2}\,\dot{m}_{\mathrm{CF}}\,\frac{R_{\mathrm{H\,I}}}{R_{\mathrm{cool}}}$$

(see O'Connell and McNamara 1989). If optically thin, the H I in 2A 0335+096 would be confined to $R_{\mathrm{H\,I}} \sim 8(T_s/100\ \mathrm{K})^{-1/2}$ kpc, with infall velocities $V_i \sim 240\ \mathrm{km\ s}^{-1}$. If the upper limit for the H I lifetime is the dynamical time, $t_{\mathrm{H\,I}} \sim R_{\mathrm{H\,I}}/V_i \lesssim 3.2 \times 10^7$ yr, the amount of H I expected to accumulate within this radius is $M_{\mathrm{H\,I}} \sim \dot{m}(R_{\mathrm{H\,I}}) \times t_{\mathrm{H\,I}} \sim 10^9\ M_\odot$. This is consistent, to within the uncertainties, with the H I upper limit for 2A 0335+096.

From the cooling flow model, the rate that H I is predicted to be deposited within the radius of the Arecibo telescope's beam, $\dot{m}(R_{\mathrm{beam}})$, is $\sim 67\%$ and $\sim 60\%$ of $\dot{m}_{\mathrm{CF}}$ for 2A 0335+096 and MKW3s, respectively. The upper limits on $M_{\mathrm{H\,I}}$ then suggest that $t_{\mathrm{H\,I}} \lesssim 3$–$10 \times 10^6$ yr, or 2–10 times smaller than the dynamical time. This value is comparable to, or somewhat less than, a stellar collapse time or the estimated lifetimes of giant molecular clouds in the Galaxy (Turner 1988).

As discussed in § III*b*, the detection of H I absorption toward MKW3s suggests that the X-ray plasma is indeed cooling to low temperatures at large radii, which is consistent with the cooling flow model. However, the model and the X-ray observations indicate that H I originating from the cooling flow should be distributed spherically about the CFD. If optically thin H I is distributed over areas as large as the observations indicate at the observed column density, it would violate the emission upper limit. This implies that the H I in MKW3s is primarily opaque. If large amounts of opaque H I are present, the H I lifetime could be larger than we have estimated by the (unknown) ratio of the masses of optically thick to optically thin H I. An additional source of uncertainty in this ratio is due to optically thin H I that may be present with a velocity width that is broadened such that its emission feature is indistinguishable from the instrumental baseline curvature. This should decrease this ratio by only $\lesssim 3$–4 times, since it is unlikely that the H I will have a velocity that is much larger than the cluster's velocity dispersion (~ 700–1000 km s^{-1}). In spite of these uncertainties, the H I upper limits exclude optically thin H I as the final repository for most of the accreting gas. Though large amounts of opaque H I may be present in cooling flows, this as well is an unlikely final repository for most of the accreting gas (see O'Connell and McNamara 1989; Loewenstein and Fabian 1990).

The H I infall velocities and line widths may provide useful constraints on models for the kinematics of cold clouds in cooling flows. Recently, Loewenstein and Fabian (1990) concluded that cold clouds should be destroyed on short time scales ($t \sim 10^4$–10^6 yr) owing to a number of mechanisms, the most important (e.g., Rayleigh-Taylor instability) being due to cloud velocities with respect to the hot gas that are of the order of the observed infall velocities and absorption-line widths. However, the H I velocities and the upper limits for $t_{\mathrm{H\,I}}$ are also

consistent with those expected for clouds forming in turbulent cooling flows. If turbulence is the primary cause of the observed H I velocities and the cold gas and hot gas are comoving, then the destructive effects of bulk motion may be reduced, increasing the cloud lifetimes to values of the order of 10^7 yr (Loewenstein and Fabian 1990).

In addition to H I, warm emission-line gas is often present in cooling flows with large mass-accretion rates. Radial gradients in the emission-line widths in cooling flow nebulae are usually consistent with infalling gas at velocities of several hundred kilometers per second (see Heckman *et al.* 1989). Although neither MKW3s or 2A 0335+096 were included in the Heckman *et al.* sample, the H I infall velocities are similar, on average, to those of the emission-line gas. In addition, the emission-line nebulae usually appear kinematically disordered, indicating that turbulent motions are important. Our H I velocity widths ($\Delta V_{\rm FWHM} \sim 35$–$100$ km s^{-1}) are much narrower than those found by Heckman *et al.* to be typical of the emission-line gas in or near the nuclei ($\Delta V_{\rm FWHM} \sim 500$–$1000$ km s^{-1}) but are closer to those found for the emission-line gas at larger radii ($\Delta V_{\rm FWHM} \sim 100$–$300$ km s^{-1}; $R \sim 5$–15 kpc). These correlations, though sketchy, suggest a possible link between the warm and cold phases of the intracluster medium, and are in qualitative agreement with our suggestion that the H I is spatially extended.

d) Cool Gas and Star Formation in CFD Galaxies

Optical and UV observations of cluster cooling flows demonstrate that $\sim 50\%$ of the well-studied CFDs have anomalously large amounts of nuclear and extended emission-line gas and extended blue colors indicative of recent or ongoing star formation at rates that are often comparable to those in disk galaxies (Wirth, Kenyon, and Hunter 1983; Hu, Cowie, and Wang 1985; Johnstone, Fabian, and Nulsen 1987; Romanishin 1987; Romanishin and Hintzen 1988; O'Connell and McNamara 1989; McNamara and O'Connell 1989). It would be useful to compare the ratio of the star formation rate to the H I mass in CFDs to that in disk galaxies. Unfortunately, the estimated star formation rates for most CFDs apply to only a small volume near the nucleus and are therefore lower limits to the total rate. Also, most upper limits to $M_{\rm H\,I}$ are not sufficiently sensitive for a meaningful statistical study (the mean H I upper limit for this sample is $\langle M_{\rm H\,I}\rangle \lesssim 6 \times 10^9\ M_\odot$ due to the large distances to most CFDs). A useful assessment of this ratio can be made, however, for 2A 0335+096, which has an estimated total star formation rate of $\dot{S} = 8\ M_\odot\ {\rm yr}^{-1}$ (Romanishin and Hintzen 1988), and a sensitive H I upper limit (see Table 1). By comparison, a typical Sb–Sc galaxy has $\dot{S} \sim 4\ M_\odot\ {\rm yr}^{-1}$ (Kennicutt 1983). In spite of their comparable star formation rates, the amount of optically thin H I in 2A 0335+096 is $\lesssim 4 \times 10^8\ M_\odot$—one or two orders of magnitude below that for a typical disk galaxy. This implies that the cool gas in 2A 0335+096 is consumed by star formation in $M_{\rm H\,I}/\dot{S} \lesssim 5 \times 10^7$ yr, which may be comparable to the lifetimes of giant molecular clouds in the Galaxy (Turner 1988) and to the H I lifetimes estimated in § IV*c*. A disk galaxy, by comparison, consumes its gas on time scales that are $\gtrsim 10^9$ yr so that cool gas is apparently consumed by star formation more efficiently in 2A 0335+096 than in disk galaxies.

e) The H I*-to-Dust Ratio in CFD Galaxies*

The hot, dense X-ray plasma in cooling flow clusters is expected to shorten the lifetime of dust due to sputtering from hot electrons, preventing a substantial buildup of dust in CFD galaxies (e.g., Hu, Cowie, and Wang 1985; Hu 1988). A few CFDs have dust lanes (e.g., 2A 0335+096 and A262), and a number of CFDs have been found to be sources of 60 μm and 100 μm emission, presumably due to dust (Bregman, McNamara, and O'Connell 1990; Grabelski and Ulmer 1990). In Table 3 we list dust masses taken from Bregman, McNamara, and O'Connell (1990) for four objects in common with this survey and give upper limits on the H I-to-dust ratio based on the H I upper limits in Table 1. Table 3 suggests that the H I–to-dust ratio for CFDs is $(M_{\rm H\,I}/M_d)_{\rm CFD} < 200$–$500$, which is consistent with the gas-to-dust ratio for the Galaxy, $(M_{\rm gas}/M_d)_{\rm GAL} \sim 100$ (Spitzer 1978).

TABLE 3

ESTIMATED UPPER LIMITS FOR H I–TO–DUST RATIOS[a]

Cluster	M_d ($10^7\ M_\odot$)	$M_{\rm H\,I}/M_d$
A262	0.25	<480
A496	1.15	<409
A1991	1.74	<207
A2063	0.50	<190
2A 0335	<1.0[b]	...

[a] Based on the H I upper limits (Table 1), and dust masses from Bregman, McNamara, and O'Connell 1990.

[b] Upper limit to dust mass assumes a dust temperature of 20 K.

It is of interest that the two objects with prominent dust lanes, A262 and 2A 0335+096, have infrared luminosities or upper limits that are similar to those CFDs without reported dust lanes. This suggests that CFDs with dust lanes may not be relatively dust-rich; rather, their dusty optical appearance could be the result of a nondispersed dust distribution.

V. SUMMARY

We conducted an H I survey of 14 cooling flow clusters and two non–cooling flow clusters with the Arecibo 1000 foot and the Green Bank 300 foot telescopes. H I absorption features were detected against the nuclear radio continuum sources of two CFDs (2A 0335+096 and MKW3s). The absorption features are broad ($\Delta V_{\rm FWHM} \sim 35$–$100$ km s^{-1}) and redshifted with respect to the stellar absorption-line velocity of the CFDs by 90–225 km s^{-1}. This indicates that the H I is falling onto, and is probably gravitationally bound to, the CFDs. The H I in the CFD 2A 0335+096 is apparently confined to a 10 kpc region of the nucleus (if the H I is optically thin), whereas the absorbing H I in MKW3s apparently lies at least 70 kpc from the nucleus of the CFD. The velocity widths of the absorption features are too broad to be accounted for by thermal Doppler broadening in a single cloud and are apparently due to $\gtrsim 45$ clouds along the line of sight. The kinematics of the H I clouds are similar to those found for the extended emission-line gas in cooling flows (see Heckman *et al.* 1989), suggesting a possible kinematic link between the warm and cold phases of the intracluster medium. If the clouds are in thermal pressure equilibrium with the hot ambient medium, the individual clouds are likely to be $\sim 3.5 \times 10^{-4}$ pc in radius, with densities of $n \sim 7 \times 10^3$ cm^{-3} and masses of $\ll 1\ M_\odot$ for a spin temperature of 100 K. These inferred cloud properties are orders of magnitude smaller in radius and mass, and larger in density than Galactic H I clouds. H I was not detected in emission; the

mean optically thin H I mass upper limit for the sample is $6 \times 10^9 M_\odot$, and the H I upper limit based on the most sensitive observations in this sample is $2 \times 10^8 M_\odot$. Upper limits to the H I–to–dust ratios (assuming the H I is optically thin) for some CFDs are consistent with the mean Galactic gas-to-dust ratio. Including NGC 1275 (Crane, van der Hulst, and Haschick 1982; Jaffe, de Bruyn, and Sijbreng 1988), there are now three CFDs with H I absorption features.

The detected CFDs have mass-accretion rates that are ~ 2.5 times larger than the CFDs that were not detected. This may indicate that the H I originated from the cooling flows. Simple radial cooling flow models, rates of star formation, and the H I upper limits yield estimates of the H I lifetime ($\lesssim 3$–15×10^6 yr) that are consistent with other relevant time scales, though the uncertainties in the estimates are large. The detection of H I in absorption toward the radio source in MKW3s may indicate that the X-ray plasma is cooling to low temperatures at a substantial fraction of the cooling radius. The large projected area of the H I in MKW3s suggested by the observations implies that the H I is optically thick. If true, considerably larger amounts of H I than indicated by our upper limit could be present. However, the H I upper limits exclude optically thin H I as the final repository for most of the accreting gas, and it is unlikely that the deficit can be accounted for, in most cases, by opaque H I.

There is a growing body of evidence that the presence of warm and cool gas and star formation in CFDs is correlated with the large cooling rates, estimated from X-ray observations, of the intracluster plasma in many clusters of galaxies. However, problems with the model remain. Among them are the cause of the large scatter in the correlations between the X-ray properties of CFD galaxies and their optical and radio (21 cm) properties, the lack of optical anomalies due to cooling at radii comparable to the cooling radius, and direct evidence for the final repository of the cooling gas. A reevaluation of these questions will be afforded by the *ROSAT* and *AXAF* X-ray observatories, which will provide high spatial resolution maps and direct temperature measurements to compare to optical and radio images. Ultraviolet observations of CFDs with the *Hubble Space Telescope* and the *ASTRO–BBXRT* missions, and ground-based CCD imaging, emphasizing the near-UV, will place strong constraints on the initial mass function, which strongly affects the radial color distribution in CFD galaxies. In addition, further efforts to obtain sensitive radio observations of the neutral and molecular gas in CFDs will constrain the possible repositories for the accreting material.

It is a pleasure to thank Kazik Borkowski, Mike Davis, Riccardo Giovanelli, Jay Lockman, Chris O'Dea, and Morton Roberts for their helpfulness and advice. We thank John Huchra, Gerard Kriss, and Riccardo Giovanelli for sharing their results in advance of publication. B. R. M. is grateful to Tom Bania for introducing him to the Arecibo telescope and especially to Craig Sarazin for many lengthy and insightful discussions. This research has been supported in part by NASA through grant NAG 5-700 and through Astrophysical Theory Program grant NAGW-764.

REFERENCES

Arnaud, K. A., and Fabian, A. C. 1989, preprint.
Bregman, J. N., McNamara, B. R., and O'Connell, R. W. 1990, *Ap. J.*, **351**, 406.
Bregman, J. N., Roberts, M. S., and Giovanelli, R. 1988, *Ap. J. (Letters)*, **330**, L93.
Burns, J. O., White, R. A., and Haynes, M. P. 1981, *A.J.*, **86**, 1120.
Caldwell, N. 1984, *Pub. A.S.P.*, **96**, 287.
Canizares, C. R., Stewart, G. C., and Fabian, A. C. 1983, *Ap. J.*, **272**, 449.
Cowie, L. L., Hu, E. M., Jenkins, E. B., and York, D. G. 1983, *Ap. J.*, **272**, 29.
Crane, P. C., van der Hulst, J. M., and Haschick, A. D. 1982, in *IAU Symposium 97, Extragalactic Radio Sources*, ed. D. S. Heeschen and C. M. Wade (Dordrecht: Reidel), p. 307.
de Vaucouleurs, G., de Vaucouleurs, A., and Corwin, H. G. 1976, *Second Reference Catalogue of Bright Galaxies* (Austin: University of Texas) (RC2).
De Young, D. S. Roberts, M. S., and Saslaw, W. C. 1973, *Ap. J.*, **185**, 809.
Faber, S. M., and Gallagher, J. S. 1976, *Ap. J.*, **204**, 365.
Fabian, A. C., ed. 1988, *Cooling Flows in Clusters and Galaxies* (Dordrecht: Kluwer).
Fabian, A. C., Nulsen, P. E. J., and Canizares, C. R. 1982, *M.N.R.A.S.*, **201**, 933.
Forman, W., and Jones, C. 1982, *Ann. Rev. Astr. Ap.*, **20**, 547.
Giovanelli, R. 1989, private communication.
Grabelski, D. A., and Ulmer, M. P. 1990, *Ap. J.*, **355**, 401.
Haynes, M. P., Brown, R. L., and Roberts, M. S. 1978, *Ap. J.*, **221**, 414.
Haynes, M. P., and Giovanelli, R. 1984, *A.J.*, **89**, 758.
Heckman, T. M. 1981, *Ap. J. (Letters)*, **250**, L59.
Heckman, T. M., Baum, S. A., van Breugel, W. J. M., and McCarthy, P. 1989, *Ap. J.*, **338**, 48.
Hu, E. M. 1988, in *Cooling Flows in Clusters and Galaxies*, ed. A. C. Fabian (Dordrecht: Kluwer), p. 73.
Hu, E. M., Cowie, L. L., and Wang, Z. 1985, *Ap. J. Suppl.*, **59**, 447.
Huchra, J. 1989, private communication.
Jaffe, W., de Bruyn, A. G., and Sijbreng, D. 1988, in *Cooling Flows in Clusters and Galaxies*, ed. A. C. Fabian (Dordrecht: Kluwer), p. 145.
Johnstone, R. M., Fabian, A. C., and Nulsen, P. E. J. 1987, *M.N.R.A.S.*, **224**, 75.
Kennicutt, R. C. 1983, *Ap. J.*, **272**, 54.
Knapp, G. R., Turner, E. L., and Cunniffe, P. E. 1985, *A.J.*, **90**, 454.
Kriss, G. A., Canizares, C. R., McClintock, J. E., and Feigelson, E. D. 1980, *Ap. J. (Letters)*, **235**, L61.
Kriss, G. A., Dixon, W. V. D., Ferguson, H. C., and Malamuth, E. M. 1989, in *Clusters of Galaxies*, ed. M. J. Fitchett and W. R. Oegerle (Baltimore: STScI), p. 129.
Kulkarni, S. R., and Heiles, C. 1988, in *Galactic and Extragalactic Radio Astronomy*, ed. G. L. Verschuur, K. I. Kellerman, and E. Bouton (Berlin: Springer), p. 95.
Lauer, T. R. 1989, preprint.
Lazareff, B., Castets, A., Kim, D. W., and Jura, M. 1989, *Ap. J. (Letters)*, **336**, L13.
Lockman, F. J., Jahoda, K., and McCammon, D. 1986, *Ap. J.*, **302**, 432.
Loewenstein, M., and Fabian, A. C. 1990, *M.N.R.A.S.*, **242**, 120.
Malumuth, E. M., and Kirshner, R. P. 1985, *Ap. J.*, **291**, 8.
McNamara, B. R., and O'Connell, R. W. 1989, *A.J.*, **98**, 2018.
McNamara, B. R., O'Connell, R. W., and Bregman, J. N. 1989, in *Clusters of Galaxies*, ed. M. J. Fitchett and W. R. Oegerle (Baltimore: STScI), p. 159.
Mirabel, I. F., Sanders, D. B., and Kazes, I. 1989, preprint.
Mushotzky, R. F., and Szymkowiak, A. E. 1988, in *Cooling Flows in Clusters and Galaxies*, ed. A. C. Fabian (Dordrecht: Kluwer), p. 53.
O'Connell, R. W., and McNamara, B. R. 1989, *A.J.*, **98**, 180.
O'Dea, C. P., and Baum, S. A. 1987, *A.J.*, **94**, 1476.
O'Dea, C. P., Baum, S. A., and Killeen, N. E. B. 1987, preprint.
O'Dea, C. P., and Owen, F. N. 1985, *A.J.*, **90**, 927.
Patnaik, A. R., and Singh, K. P. 1988, *M.N.R.A.S.*, **234**, 847.
Romanishin, W. 1987, *Ap. J. (Letters)*, **323**, L113.
Romanishin, W., and Hintzen, P. 1988, *Ap. J. (Letters)*, **324**, L17.
Sarazin, C. L. 1986, *Rev. Mod. Phys.*, **58**, 1.
Sarazin, C. L., and O'Connell, R. W. 1983, *Ap. J.*, **268**, 552.
Savage, B. D., and Mathis, J. S. 1979, *Ann. Rev. Astr. Ap.*, **17**, 73.
Schwartz, D. A., Schwarz, J., and Tucker, W. 1980, *Ap. J. (Letters)*, **238**, L59.
Singh, K. P., Westergaard, N. J., and Schnopper, H. W. 1988, *Ap. J.*, **331**, 672.
Slingo, A. 1974, *M.N.R.A.S.*, **168**, 307.
Spitzer, L. 1978, *Physical Processes in the Interstellar Medium* (New York: Wiley).
Struble, M. F., and Rood, H. J. 1987, *Ap. J. Suppl.*, **63**, 543.
Thomas, P. A., Fabian, A. C., and Nulsen, P. E. J. 1987, *M.N.R.A.S.*, **228**, 973.
Turner, B. 1988, in *Galactic and Extragalactic Radio Astronomy*, ed. G. L. Verschuur, K. I. Kellerman, and E. Bouton (Berlin: Springer), p. 154.

Valentijn, E. A., and Giovanelli, R. 1982, *Astr. Ap.*, **114**, 208.
Van Gorkom, J. H., Knapp, G. R., Ekers, R. D., Ekers, D. D., Laing, R. A., and Polk, K. S. 1989, preprint.
Westergaard, N. J. 1988, in *Cooling Flows in Clusters and Galaxies*, ed. A. C. Fabian (Dordrecht: Kluwer), p. 165.
White, R. E., and Sarazin, C. L. 1988, *Ap. J.*, **335**, 688.
Wirth, A., Kenyon, S. J., and Hunter, D. A. 1983, *Ap. J.*, **269**, 102.
Zhao, J-H., Burns, J. O., and Owen, F. N. 1989, *A.J.*, **98**, 64.

JOEL N. BREGMAN: Astronomy Department, University of Michigan, Dennison Building, Ann Arbor, MI 48109-1090

BRIAN R. MCNAMARA and ROBERT W. O'CONNELL: Astronomy Department, University of Virginia, P.O. Box 3818, Charlottesville, VA 22903